Spin-Wave Doppler Shift by Magnon Drag in Magnetic Insulators

Tao Yu,[1] Chen Wang,[2] Michael A. Sentef,[1] and Gerrit E. W. Bauer[3]

[1]*Max Planck Institute for the Structure and Dynamics of Matter,*
Luruper Chaussee 149, 22761 Hamburg, Germany
[2]*Center for Joint Quantum Studies and Department of Physics,*
School of Science, Tianjin University, Tianjin 300350, China
[3]*Institute for Materials Research & WPI-AIMR & CSRN, Tohoku University, Sendai 980-8577, Japan*
(Dated: December 1, 2020)

Doppler shift of quasiparticle dispersion induced by charge currents is responsible for the critical supercurrents in superconductors and spin-wave instabilities by spin-transfer torque in metallic ferromagnets. Here we predict an analogous effect in thin films of magnetic insulators. A coherent spin current, excited by stripline microwaves, or a thermal magnon current, driven by a temperature gradient, can induce a Doppler shift that tilts the magnon dispersion in the spin-current direction. Around a critical driving strength, that is characterized by a spin-wave instability in the self-consistent mean-field treatment, the pumped magnon current reaches a maximum accompanied by a strong breaking of chiral pumping. The backaction of magnon currents on magnetic orders is therefore important for realizing large spin currents in low-dimensional magnonic devices.

Introduction.—Electrically insulating magnetic films hold the promise of low-dissipation information processing with magnons [1–5]. Complex nonlinear dynamics emerge in the presence of a large number of nonequilibrium magnons [6, 7], excited by microwaves [8–10], heating [11, 12], or electrical spin injection [13–15]. The nonequilibrium magnon chemical potential can overcome the magnon gap to cause magnon Bose-Einstein condensation [8, 14, 16–18]. The presently most suitable material to study magnon dynamics is yttrium iron garnet (YIG), a ferrimagnet with high Curie temperature and arguably the lowest damping [19, 20]. Ultrathin YIG films with thicknesses even below 10 nm can maintain very high magnetic quality [21, 22] and a strongly enhanced magnon conductivity [14, 15]. Magnons in thin films of YIG injected via current-biased platinum contacts through the spin Hall effect enhance the Drude-type magnon conductivity [13, 14, 23], affect the magnon chemical-potential distribution [24], or lead to Bose-Einstein condensation [14, 25, 26].

Realizing large spin current is an important pursuit in spintronics. In *metallic* ferromagnets, electric currents excite magnetization dynamics by the spin-transfer torque [27, 28]. The charge current induces a Doppler shift, i.e., a tilt of the spin-wave dispersion of a homogeneous magnetization in momentum space, which could trigger a spin-wave instability [29–31] and modulate the magnetic ground state [32]. In superconductors the critical supercurrent is caused by the Doppler shift of Bogoliubov quasiparticles. These obviously do not apply to magnetic insulators that cannot carry an electric charge current. However, magnetic insulators are also conduits for (magnonic) spin currents. By solving the self-consistent problem of a magnon gas interacting with its own current, we find that magnon spin currents can also affect the magnon dispersion via a Doppler effect.

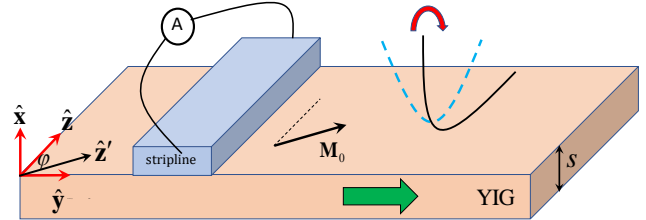In this Letter, we formulate the dynamics of long-

FIG. 1. (Color online) Magnonic Doppler effect of thin magnetic films driven by pure magnon current. A long stripline along the $\hat{\mathbf{z}}$-direction is illustrated to pump the magnon current (the green thick arrow) in YIG films of thickness s that causes the tilt of magnon dispersion, as shown by the red thick arrow and parabolic bands. The in-plane magnetization is saturated with a relative angle φ to the stripline direction.

wavelength coherent magnons of thin YIG films in the presence of large magnon currents that are pumped by stripline microwaves, as depicted in Fig. 1, or injected thermally or electrically via Pt contacts. We predict an interaction-induced drag effect, in the form of a magnonic Doppler effect, on the magnon velocities, that tilts the spin-wave dispersion. The associated physics differs strongly from the magnon-drag by phonon [33] or electron [29–31, 34] currents by its nonlinearity origin. Its phenomenology is intriguingly similar to an interfacial Dzyaloshinskii-Moriya interaction (DMI) [35–37]. The polarization-momentum locked AC magnetic field emitted by a microwave stripline [38–40] coherently populates magnon states at one side of the stripline through the chiral pumping effect, with a unidirectional magnon current that simultaneously modifies the magnon dispersion. Incoherent magnon accumulations injected thermally or electrically propagate diffusely and generate a magnon current proportional to their density gradient. At a critical value of any of these, the magnon excitation energy

touches zero at a particular momentum, indicating an instability of the ground state with constant magnetization. Around this critical driving, we predict a maximum of the magnonic spin current accompanied with a strong breaking of the chirality in magnetization excitation by striplines. Our work points out the importance of the backaction of magnon currents on magnetic orders in the realization of large spin currents in magnetic insulators, providing a different scenario to the nonlinearity by populations.

Model and formalism.—We consider an in-plane magnetized YIG film with thickness $s = \mathcal{O}(10)$ nm, with surface normal oriented along the $\hat{\mathbf{x}}$-direction. An in-plane static magnetic field $\mathbf{H}_{\mathrm{app}}$ is applied at an angle φ to the stripline $\hat{\mathbf{z}}$-direction (Fig. 1). The Hamiltonian of the magnetic order reads

$$\hat{H} = \mu_0 \int \left(\frac{\alpha_{\mathrm{ex}}}{2} (\nabla \hat{\mathbf{M}})^2 - \hat{\mathbf{M}} \cdot \mathbf{H}_{\mathrm{app}} \right) d\mathbf{r}, \qquad (1)$$

where μ_0 is the vacuum permeability, α_{ex} is the exchange stiffness, and $\mathbf{M}$ is the magnetization. We disregard anisotropies [41, 42] because the crystal ones are small in YIG, while the dipolar ones are strongly suppressed in the thin film limit [43, 44]. The exchange length in YIG is $\lambda_{\mathrm{ex}} = 2\pi\sqrt{\alpha_{\mathrm{ex}}} = 109$ nm since $\alpha_{\mathrm{ex}} = 3 \times 10^{-16}$ m^2 [45, 46]. The magnetization dynamics then obeys a Landau-Lifshitz-Gilbert (LLG) equation

$$\frac{d\mathbf{M}}{dt} = -\mu_0\gamma\mathbf{M} \times (\mathbf{H}_{\mathrm{app}} + \alpha_{\mathrm{ex}}\nabla^2\mathbf{M}) + \frac{\alpha_G}{M_s}\mathbf{M} \times \frac{d\mathbf{M}}{dt}, \quad (2)$$

where α_G is the Gilbert damping constant and $-\gamma$ is the electron gyromagnetic ratio. In the absence of external torques and damping the magnetization carries a magnetization current density

$$\tilde{\mathbf{j}} = -(1/2)\alpha_{\mathrm{ex}}\mu_0\mathbf{M} \times \nabla\mathbf{M} \qquad (3)$$

that satisfies the continuity equation $d\mathbf{M}/dt + \nabla \cdot \tilde{\mathbf{j}} = 0$ [47].

The LLG phenomenology contains all of the nonlinearities that can be captured by interacting magnons to some extent. The Holstein-Primakoff transformation expresses the magnetization dynamics by bosonic magnon operators $\hat{\Theta}(\mathbf{r})$ with $\hat{S}_x(\mathbf{r}) + i\hat{S}_{y'}(\mathbf{r}) = \hat{\Theta}^\dagger(\mathbf{r})\sqrt{2S - \hat{\Theta}^\dagger(\mathbf{r})\hat{\Theta}(\mathbf{r})}$ and $\hat{S}_{z'}(\mathbf{r}) = -S + \hat{\Theta}^\dagger(\mathbf{r})\hat{\Theta}(\mathbf{r})$, where the spin operators $\hat{\mathbf{S}} = -\mathbf{M}/(\gamma\hbar)$. The leading terms in the expansion of the square roots leads to a complete set of harmonic oscillators, that we use to expand the full problem. The eigenmodes normal to the film plane depend on the boundary conditions, that become free for thin films [48]. The magnon operators in position space can then be expanded in perpendicular standing spin waves (PSSWs) with index l [43, 44]

$$\hat{\Theta}(\mathbf{r}) = \sum_{l \geq 0} \sqrt{\frac{2}{1 + \delta_{l0}}} \frac{1}{\sqrt{s}} \cos\left(\frac{l\pi}{s}x\right) \hat{\Psi}_l(\boldsymbol{\rho}). \qquad (4)$$

Substituting these expressions into the Holstein-Primakoff expansion, the Hamiltonian can be written as $\hat{H} = \hat{H}_{\mathrm{L}} + \hat{H}_{\mathrm{NL}} + \cdots$, where $\hat{H}_{\mathrm{L}}$ describes the non-interacting magnon gas and $\hat{H}_{\mathrm{NL}}$ is the leading nonlinear term that introduces interactions between the magnons. At sufficiently low magnon densities

$$\hat{H} \to \hat{H}_{\mathrm{L}} = \sum_l (E_l + \hbar\omega_M\alpha_{\mathrm{ex}}k^2) \int \hat{\Psi}_l^\dagger(\boldsymbol{\rho})\hat{\Psi}_l(\boldsymbol{\rho})d\boldsymbol{\rho}, \quad (5)$$

where $E_l = \mu_0\gamma\hbar H_{\mathrm{app}} + \hbar\omega_M\alpha_{\mathrm{ex}}(l\pi/s)^2$ is the edge of the l-th band with $\omega_M \equiv \mu_0\gamma M_s$. The nonlinear Hamiltonian

$$\hat{H}_{\mathrm{NL}} = \sum_{l_i} \mathcal{U}_{l_1l_2l_3l_4} \int \hat{\Psi}_{l_1}^\dagger(\boldsymbol{\rho})\hat{\Psi}_{l_2}^\dagger(\boldsymbol{\rho})\hat{\Psi}_{l_3}(\boldsymbol{\rho})\hat{\Psi}_{l_4}(\boldsymbol{\rho})d\boldsymbol{\rho}$$

$$+ \sum_{l_i} \mathcal{V}_{l_1l_2l_3l_4} \int \hat{\Psi}_{l_1}^\dagger(\boldsymbol{\rho})\hat{\Psi}_{l_2}^\dagger(\boldsymbol{\rho})\nabla_{\boldsymbol{\rho}}\hat{\Psi}_{l_3} \cdot \nabla_{\boldsymbol{\rho}}\hat{\Psi}_{l_4}d\boldsymbol{\rho} + \mathrm{H.c.}$$

contains two types of magnon-number conserving interactions derived in the Supplemental Material [49]. The potentials are governed by magnon-mode overlap integrals

$$\mathcal{U}_{l_1l_2l_3l_4} = \frac{\mu_0\gamma^2\hbar^2\alpha_{\mathrm{ex}}l_3l_4\pi^2\mathcal{A}_{l_1l_2l_3l_4}}{s^3\sqrt{(1 + \delta_{l_10})(1 + \delta_{l_20})(1 + \delta_{l_30})(1 + \delta_{l_40})}},$$

$$\mathcal{V}_{l_1l_2l_3l_4} = \frac{\mu_0\gamma^2\hbar^2\alpha_{\mathrm{ex}}\mathcal{B}_{l_1l_2l_3l_4}}{s\sqrt{(1 + \delta_{l_10})(1 + \delta_{l_20})(1 + \delta_{l_30})(1 + \delta_{l_40})}},$$

with dimensionless form factors

$$\mathcal{A}_{l_1l_2l_3l_4} = \frac{1}{s}\int_{-s}^0 dx\,\Pi_{i=1,2}\cos\left(\frac{l_i\pi}{s}x\right)\Pi_{j=3,4}\sin\left(\frac{l_j\pi}{s}x\right),$$

$$\mathcal{B}_{l_1l_2l_3l_4} = \frac{1}{s}\int_{-s}^0 dx\,\Pi_{i=1,2,3,4}\cos\left(\frac{l_i\pi}{s}x\right).$$

When $l_1 = 0$, the scattering potentials obey selection rules $\mathcal{U}_{0l_2l_3l_4} \propto l_3l_4(\delta_{l_2+l_3,l_4} + \delta_{l_2+l_4,l_3} - \delta_{l_3+l_4,l_2})$ and $\mathcal{V}_{0l_2l_3l_4} \propto (\delta_{l_2+l_3,l_4} + \delta_{l_2+l_4,l_3} + \delta_{l_2+l_3+l_4,0} + \delta_{l_3+l_4,l_2})$. In the strictly two-dimensional limit, $\mathcal{U}_{0000} = 0$ vanishes, but $\mathcal{V}_{0000} = \mathcal{V}_{00ll} = \mathcal{V}_0 = \mu_0\gamma^2\hbar^2\alpha_{\mathrm{ex}}/(4s)$ is large. The divergence for vanishing film thickness is an artifact of the continuum approximation that breaks down when s approaches unit cell dimensions.

We are interested in the effect of a magnon current on a low-frequency coherent excitation, i.e., at excitation frequency $\omega/(2\pi) \lesssim 1$ GHz, which allows us to set $l_1 = 0$. Using the above selection rules of the scattering potentials and energy conservation, we prove in the Supplemental Material [49] that the incoherent scattering of these *low-energy* magnons by those in all other bands is marginally small. The leading nonlinearities in the coherent magnon states thus reduce to a self-consistent mean-field problem [50, 51], in which the interaction renormalizes the energy dispersion but does not affect magnon dephasing and lifetime. The coherent magnon amplitude

in the lowest band obeys a Heisenberg equation of motion that is augmented by the Gilbert damping [49],

$$i\hbar(1 - i\alpha_G)\frac{\partial\langle\hat\Psi_0(\boldsymbol\rho)\rangle}{\partial t} = E_0\langle\hat\Psi_0(\boldsymbol\rho)\rangle - \hbar\omega_M\alpha_{\rm ex}\nabla^2\langle\hat\Psi_0(\boldsymbol\rho)\rangle$$

$$+ \frac{8i}{\hbar}\sum_{l'\geq 0}\mathcal{V}_{00l'l'}\mathbf{J}_{l'}(\boldsymbol\rho)\cdot\nabla_{\boldsymbol\rho}\langle\hat\Psi_0(\boldsymbol\rho)\rangle + P_{\rm ex}, \qquad (6)$$

where $\langle\cdots\rangle$ represents an ensemble average,

$$\mathbf{J}_l(\boldsymbol\rho) = \frac{\hbar}{2i}\left(\langle\hat\Psi_l^\dagger(\boldsymbol\rho)\nabla_{\boldsymbol\rho}\hat\Psi_l(\boldsymbol\rho)\rangle - \langle\hat\Psi_l(\boldsymbol\rho)\nabla_{\boldsymbol\rho}\hat\Psi_l^\dagger(\boldsymbol\rho)\rangle\right) \quad (7)$$

is the linear-momentum magnon current density in sub-band l with contributions from both coherent and incoherent magnons, and $P_{\rm ex}$ is a microwaves excitation source that will be specified below. The (locally) uniform magnon current hence engages the gradient (or momentum) of the magnon amplitude $\nabla_{\boldsymbol\rho}\langle\hat\Psi_0\rangle$ and tilts the magnon dispersion, which is an interaction-induced drag effect [33, 34]. This drag depends only on the magnitude of the current, not on the coherent versus incoherent nature of the carriers.

The magnon linear-momentum current density [Eq. (7)] is proportional to the magnon number current density $\tilde{\mathbf{J}}_l$ defined by the continuity equation and the Heisenberg equation of motion for the non-interacting magnon Hamiltonian, since the exchange magnons have a constant mass $\hbar/(2\omega_M\alpha_{\rm ex})$. The former is also a spin current since in the absence of anisotropies the magnons carry angular momentum $\hbar$. With magnon density operator $\hat\rho_m^l(\boldsymbol\rho) = \langle\hat\Psi_l^\dagger(\boldsymbol\rho)\hat\Psi_l(\boldsymbol\rho)\rangle$

$$\frac{\partial\hat\rho_m^l(\boldsymbol\rho)}{\partial t} = \frac{1}{i\hbar}[\hat\rho_m^l(\boldsymbol\rho), \hat{H}_{\rm L}] = -\nabla\cdot\tilde{\mathbf{J}}_l(\boldsymbol\rho), \qquad (8)$$

leading to $\left\langle\tilde{\mathbf{J}}_l(\boldsymbol\rho)\right\rangle = (2\omega_M\alpha_{\rm ex}/\hbar)\mathbf{J}_l(\boldsymbol\rho)$, which is consistent with Eq. (3) since $1/(\gamma\hbar)\int dx\tilde{\mathbf{j}}(x,\boldsymbol\rho)\to\tilde{\mathbf{J}}_l(\boldsymbol\rho)$ when $l = 0$ to linear order in the magnon operator.

Magnonic Doppler effect.—The microwaves emitted by a long stripline on top of a thin magnetic film launch a coherent magnon current normal to it. We consider a metallic wire of rectangular cross section $0 < x < d$ and $-w/2 < y < w/2$ (Fig. 1) with an AC current density I of frequency ω_s. The microwaves are uniform over the film thickness when $s \ll d$. The Fourier component k_y of the Oersted magnetic field in the thin film below the stripline ($x \to -s/2$) reads [38–40, 52–54],

$$H_x(k_y, \omega_s) = i\frac{I(\omega_s)}{2}\mathcal{F}(d,w)\mathrm{sgn}(k_y)e^{-|k_y|(d+s)/2},$$

$$H_y(k_y, \omega_s) = -\frac{I(\omega_s)}{2}\mathcal{F}(d,w)e^{-|k_y|(d+s)/2}, \qquad (9)$$

with $\mathcal{F}(d,w) = (2/k_y^2)\sin(k_y w/2)\left(1 - e^{-|k_y|d}\right)$ determined by stripline dimensions. Here we used $|k_y| \gg \omega_s/c$ because the velocity of light c is much larger than that of the magnons. The magnetic field $H_y(k_y, \omega_s) = i\mathrm{sgn}(k_y)H_x(k_y, \omega_s)$ is right and left circularly polarized for positive and negative k_y, respectively, so polarization and momentum are locked. This field couples to the magnons of the lowest PSSW band up to wave numbers $k_y \sim \pi/w$ by the Zeeman interaction

$$\hat{H}_{\rm Z} = g\sum_{k_y}\left(H_x(k_y, t) - i\cos\varphi H_y(k_y, t)\right)\hat\Psi_0^\dagger(k_y) + \mathrm{H.c.},$$

with coupling constant $g = \mu_0\sqrt{\gamma\hbar M_s s/2}$, so the excitation source $P_{\rm ex} = g(H_x(k_y, t) - i\cos\varphi H_y(k_y, t))$ in Eq. (6). The in-plane magnetization angle φ can be rotated by an applied DC magnetic field to tune the magnitude and direction of the pumped magnon current. When $\varphi = 0$, the stripline magnetic field launches a magnon current with $k_y > 0$ into half space (see below). Thereby the excited magnon current $\mathbf{J}_y(y > 0) = \overline{\mathbf{J}}_y\exp(-y/\delta)$ decays exponentially with distance from the source on the scale of the decay length $\delta(\omega_s) \sim 2/\mathrm{Im}\,\kappa_y \sim \sqrt{(\alpha_{\rm ex}\omega_M)(\omega_s - \mu_0\gamma H_{\rm app})}/(\alpha_G\omega_s)$, i.e. the root of $(\omega_s - \mu_0\gamma H_{\rm app} - \omega_M\alpha_{\rm ex}\kappa_y^2)^2 + (\alpha_G\omega_s)^2 = 0$. On the other hand, the amplitude $\langle\hat\Psi_0(\boldsymbol\rho)\rangle$ oscillates rapidly with wavelength $(1/|\kappa_y| \ll \delta)$. Near the stripline, the magnon current in the lowest band obeys the integral equation, obtained from Eq. (6),

$$\overline{\mathbf{J}}_y = \frac{1}{\delta}\left(\frac{g}{\hbar}\right)^2\int\frac{dk_y}{2\pi}k_y\frac{|H_x(k_y) - iH_y(k_y)|^2}{(\omega_s - \tilde\omega_{k_y})^2 + \alpha_G^2\omega_s^2}, \qquad (10)$$

with Doppler-shifted magnon frequency

$$\tilde\omega_{\mathbf{k}} = \mu_0\gamma H_{\rm app} + \omega_M\alpha_{\rm ex}k^2 - (8/\hbar^2)\mathcal{V}_0 k_y\overline{\mathbf{J}}_y, \qquad (11)$$

which can be solved iteratively or graphically.

A magnon current can also be carried by the incoherent thermal magnons driven by a magnon chemical potential or temperature gradient. These can be created either by the spin-Hall effect in, or Ohmic heating of, current-biased Pt contacts [13, 14]. We can estimate the steady-state magnon current under a temperature gradient ∇T by the linearized Boltzmann equation in the relaxation-time approximation [23, 50, 55], assuming that the drag term in the collision integral is small,

$$-\mathbf{v}_{\mathbf{k},l}\cdot\nabla T\frac{\partial f_{\mathbf{k},l}}{\partial T} = -\frac{f_{\mathbf{k},l} - f_{\mathbf{k},l}^{(0)}}{\tau_{\mathbf{k},l}}, \qquad (12)$$

where $\mathbf{v}_{\mathbf{k},l} = (1/\hbar)\partial E_l(\mathbf{k})/\partial\mathbf{k} = 2\omega_M\alpha_{\rm ex}\mathbf{k}$ is the magnon group velocity, $f_{\mathbf{k},l} = \langle\hat\Psi_l^\dagger(\mathbf{k})\hat\Psi_l(\mathbf{k})\rangle$ is the magnon distribution in the l-band, $f_{\mathbf{k},l}^{(0)} = 1/\{\exp[E_{\mathbf{k},l}/(k_B T)] - 1\}$ is the equilibrium Planck distribution at temperature T, $\tau_{\mathbf{k},l} \approx \hbar/(\alpha_G E_{\mathbf{k},l})$ is the magnon relaxation time [23]. Assuming a uniform $\nabla T = \mathcal{E}_y\hat{\mathbf{y}}$ applied along the $\hat{\mathbf{y}}$-direction, the magnon momentum current [Eq. (7)]

$$\mathbf{J}_y = \hbar\omega_M\alpha_{\rm ex}\mathcal{E}_y\int\frac{dk_y dk_z}{2\pi^2}k_y^2\sum_{l\geq 0}\tau_{\mathbf{k},l}\frac{\partial f_{\mathbf{k},l}^{(0)}}{\partial T}, \qquad (13)$$

which also causes a Doppler shift [Eq. (11)] of the coherent magnon amplitude.

Figure 2(a) illustrates the pumped magnon current $\overline{\mathbf{J}}_y$ as a function of the applied electric current density I with frequency $\omega_s/(2\pi) \approx 0.93$ GHz across the stripline of width $w = 150$ nm and thickness $d = 80$ nm [21, 54] from Eq. (10) in comparison with numerical solutions of the LLG equation [Eq. (3)]. Here the YIG film
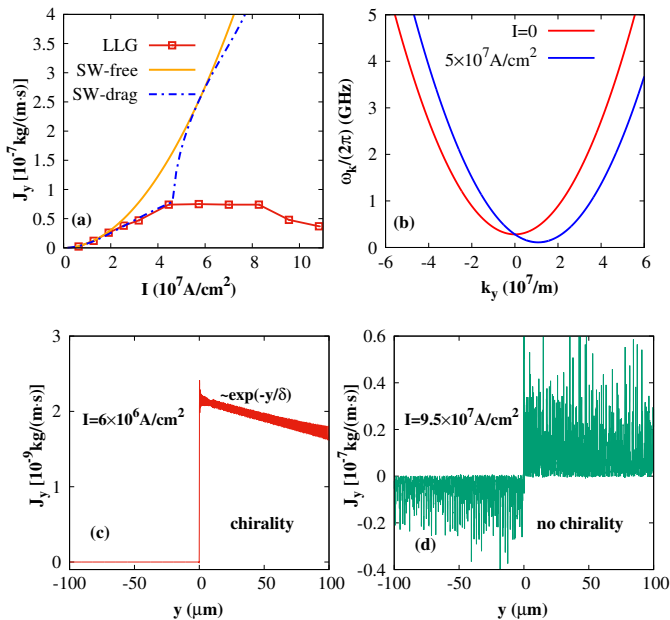

FIG. 2. (Color online) Magnon currents and Doppler shift of magnon dispersion under stripline microwave excitation. (a) shows the coherently pumped magnon current $\overline{\mathbf{J}}_y$ as a function of the applied electric current density I in the stripline from numerical LLG calculations ("LLG"), non-interacting spin-wave theory ("SW-free"), and spin-wave theory including the drag effect ("SW-drag"). The tilt of magnon dispersion at high excitation is illustrated in (b). We illustrate the chirality of the spin-current excitation for $I < I_c$ [(c)] and $I > I_c$ [(d)], respectively. The parameters used in the calculations are given in the text and figures.

thickness $s = 10$ nm, the applied static magnetic field $\mu_0 H_{\mathrm{app}} = 10$ mT that drives out domain walls [21, 46], $\mu_0 M_s = 0.18$ T, and $\alpha_G = 10^{-4}$. Magnons of wavelength $2w$ are resonantly excited and carry a current with decay length $\delta \approx 333$ μm. Here we compare the analytical solutions with the numerically exact solution of the LLG equation, which predicts a maximum spin-wave current for a stripline current $I_c \approx 5 \times 10^7$ A/cm². The non-interacting spin-wave theory (SW-free) fails already for small I, which emphasizes the importance of nonlinearities. When including the drag effect, the spin-wave theory Eq. (10) $\overline{\mathbf{J}}_y$ saturates at a current $I \sim I_c$, but returns to the non-interacting values at larger currents. I_c is determined by the onset of a spin-wave instability that is characterized by negative magnon excitation energy (see

below), which causes the discontinuous change of the spin current calculated by the self-consistent mean-field theory. When $I > I_c$, the lowest-order nonlinearity of the Holstein-Primakoff expansion and thereby the mean-field theory may break down. The Doppler shift of the spin-wave dispersion illustrated in Fig. 2(b) holds only for $I < I_c$. When $I \gtrsim I_c$, we observe that the chirality of the magnon excitation is strongly reduced, indicating that the backscattering of magnons becomes strong, as illustrated by Figs. 2(c) and (d), which is partly responsible for the suppression of spin current at strong driving.

A maximum value of the spin current in ultrathin YIG films was observed in a transistor in which a DC-current biased Pt gate injects magnons into the conducting channel [15]. Here we find in the coherent excitation regime that the magnon nonlinearity naturally limits the spin current to a maximum. The tilt of dispersion causes chiral velocities of spin waves of the same energy that should be observable by changes in the microwave transmission [21, 46], nitrogen-vacancy center magnetometry [54, 56], and Brillouin light scattering [57]. The dispersion tilts into the opposite direction when the magnetization direction is reversed ($\varphi = \pi$) and vanishes when perpendicular to the stripline ($\varphi = \pi/2$), i.e., it follows the current direction governed by the chirality of the stripline magnetic field. The basic features agree with recently reported experiments in YIG thin films of thickness $s = 7$ nm [21] that were interpreted in terms of the DMI by spin-orbit interaction. A significant DMI has been reported for the interface between GGG and rare earth iron garnets [58], but has not yet been confirmed by other studies on YIG|GGG, to the best of our knowledge.

Magnetization chirality breaking.—We trace a close connection between the broken magnetization chirality and spin-wave instability, within the mean-field theory. Negative excitation energies of quasiparticles at finite momenta imply an instability of the ground state [29, 30, 32]. According to Eq. (11) a critical magnon current $\mathbf{J}_y^{(c)}$ generated by incoherent pumping can cause negative magnon excitation energies $\tilde{E}_0(\mathbf{k}) < 0$ at the momentum $k_y^{(c)} = 4\mathcal{V}_0 \overline{\mathbf{J}}_y/(\hbar^2 \omega_M \alpha_{\mathrm{ex}})$, when the magnon current is larger than a critical value

$$\mathbf{J}_y^{(c)} = \hbar/(4\mathcal{V}_0)\sqrt{\hbar \omega_M \alpha_{\mathrm{ex}} E_0}. \tag{14}$$

With the above YIG parameters, the critical magnon current $\mathbf{J}_y^{(c)} \approx 10^{-7}$ kg/(m·s). This value can be reached by incoherent spin injection with a critical temperature gradient $\mathcal{E}_y^{(c)} \approx 4$ K/μm when $T = 300$ K [Eq. (13)]. By stripline microwave excitation the critical spin current density is predicted when $I \sim I_c$ by the drag theory. However, according to the LLG calculations in Fig. 2(a) nonlinearities might prohibit reaching this critical value.

Around the spin-wave instability driving strength I_c the magnetization at one side of the stripline reaches its maximum with a rapid increase of the magnetization at

the other side. Figure 3 shows the suppression of chirality under strong excitation. The nonequilibrium magnetization for $y > 0$ is maximal around I_c, at which magnons accumulate also at $y < 0$. The chirality is strongly broken at a stronger driving with nearly equal excited magnetizations at the two sides of the stripline. We note the analogy with a magnetic domain wall centered at the stripline [32]. Under high excitation the injected power propagates in both directions, similar to the electric or thermal injection of an incoherent magnon accumulation. Chirality of magnetization is thereby a measure of magnon backscattering, which should be protected topologically for magnetostatic surface magnons [59].
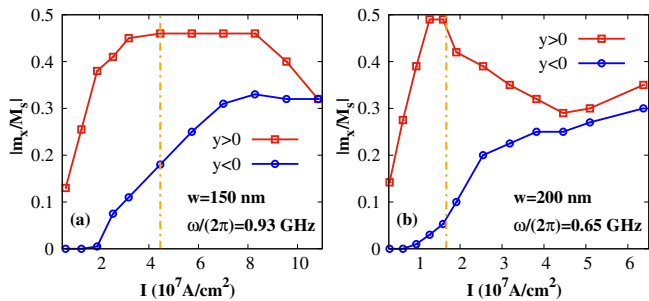

FIG. 3. (Color online) Suppressed chirality by nonlinearity at excitation frequencies $\omega_s = 2\pi \times 0.93$ GHz [(a)] and $2\pi \times 0.65$ GHz [(b)]. Orange dot-dashed line indicates I_c at different conditions. The parameters used in the calculations are given in the text and figures.

Discussion.—Large spin currents can realize efficient spin transport that needs strong driving of the magnetic orders. We formulated the response of a ferromagnet to strong driving and found a Doppler shift of magnon dispersion by a magnon-interaction-driven drag effect. It requires a stripline current density $\sim 2 \times 10^7$ A/cm^2 in one or $\sim (2/\mathcal{N}) \times 10^7$ A/cm^2 in $\mathcal{N}$ striplines over a total width that should be small compared to the magnon propagation length, i.e., many micrometers. The chiral velocities here are controllable by the stripline chirality, which was observed at a YIG|GGG interface [21]. The nonmonotonic dependence of the spin current response to the microwave power might be related to the nonmonotonicity in nonlocal spin wave transport as a function of spin injection by a Pt gate [14, 15]. Our study helps to realize large magnon spin currents and understand their effects on the magnetic orders in magnetic insulators.

[1] B. Lenk, H. Ulrichs, F. Garbs, and M. Muenzenberg, Phys. Rep. **507**, 107 (2011).
[2] A. V. Chumak, V. I. Vasyuchka, A. A. Serga, and B. Hillebrands, Nat. Phys. **11**, 453 (2015).
[3] D. Grundler, Nat. Nanotechnol. **11**, 407 (2016).
[4] V. E. Demidov, S. Urazhdin, G. de Loubens, O. Klein, V. Cros, A. Anane, and S. O. Demokritov, Phys. Rep. **673**, 1 (2017).
[5] A. Brataas, B. van Wees, O. Klein, G. de Loubens, and M. Viret, Phys. Rep. **885**, 1 (2020).
[6] P. W. Anderson and H. Suhl, Phys. Rev. **100**, 1788 (1955).
[7] V. S. L'vov, *Wave Turbulence Under Parametric Excitation* (Springer-Verlag Berlin Heidelberg, 1994).
[8] S. O. Demokritov, V. E. Demidov, G. A. Melkov, A. A. Serga, B. Hillebrands, and A. N. Slavin, Nature (London) **443**, 430 (2006).
[9] J. Liu, F. Feringa, B. Flebus, L. J. Cornelissen, J. C. Leutenantsmeyer, R. A. Duine, and B. J. van Wees, Phys. Rev. B **99**, 054420 (2019).
[10] C. Du, T. V. der Sar, T. X. Zhou, P. Upadhyaya, F. Casola, H. Zhang, M. C. Onbasli, C. A. Ross, R. L. Walsworth, Y. Tserkovnyak, and A. Yacoby, Science **357**, 195 (2017).
[11] E. Padroń-Hernańdez, A. Azevedo, and S. M. Rezende, Phys. Rev. Lett. **107**, 197203 (2011).
[12] J. Cramer, L. Baldrati, A. Ross, M. Vafaee, R. Lebrun, and M. Kläui, Phys. Rev. B **100**, 094439 (2019).
[13] L. J. Cornelissen, J. Liu, B. J. van Wees, and R. A. Duine, Phys. Rev. Lett. **120**, 097702 (2018).
[14] T. Wimmer, M. Althammer, L. Liensberger, N. Vlietstra, S. Geprägs, M. Weiler, R. Gross, and H. Huebl, Phys. Rev. Lett. **123**, 257201 (2019).
[15] J. Liu, X.-Y. Wei, G. E. W. Bauer, J. Ben Youssef, and B. J. van Wees, arXiv:2011.07800.
[16] L. Berger, Phys. Rev. B **54**, 9353 (1996).
[17] S. A. Bender, R. A. Duine, A. Brataas, and Y. Tserkovnyak, Phys. Rev. B **90**, 094409 (2014).
[18] B. Flebus, S. A. Bender, Y. Tserkovnyak, and R. A. Duine, Phys. Rev. Lett. **116**, 117201 (2016).
[19] H. Chang, P. Li, W. Zhang, T. Liu, A. Hoffmann, L. Deng, and M. Wu, IEEE Magn. Lett. **5**, 6700104 (2014).
[20] V. Cherepanov, I. Kolokolov, and V. L'vov, Phys. Rep. **229**, 81 (1993).
[21] H. C. Wang, J. L. Chen, T. Liu, J. Y. Zhang, K. Baumgaertl, C. Y. Guo, Y. H. Li, C. P. Liu, P. Che, S. Tu, S. Liu, P. Gao, X. F. Han, D. P. Yu, M. Z. Wu, D. Grundler, and H. M. Yu, Phys. Rev. Lett. **124**, 027203 (2020).
[22] J. Mendil, M. Trassin, Q. Bu, J. Schaab, M. Baumgartner, C. Murer, P. T. Dao, J. Vijayakumar, D. Bracher, C. Bouillet, C. A. F. Vaz, M. Fiebig, and P. Gambardella, Phys. Rev. Mat. **3**, 034403 (2019).
[23] L. J. Cornelissen, K. J. H. Peters, G. E. W. Bauer, R. A. Duine, and B. J. van Wees, Phys. Rev. B **94**, 014412 (2016).
[24] C. Ulloa, A. Tomadin, J. Shan, M. Polini, B. J. van Wees, and R. A. Duine, Phys. Rev. Lett **123**, 117203 (2019).
[25] S. A. Bender, R. A. Duine, A. Brataas, and Y. Tserkovnyak, Phys. Rev. B **90**, 094409 (2014).
[26] R. E. Troncoso, A. Brataas, and R. A. Duine, Phys. Rev. B **99**, 104426 (2019).

[27] S. Zhang and Z. Li, Phys. Rev. Lett. **93**, 127204 (2004).

[28] Y. Tserkovnyak, H. J. Skadsem, A. Brataas, and G. E. W. Bauer, Phys. Rev. B **74**, 144405 (2006).

[29] Ya. B. Bazaliy, B. A. Jones, and S.-C. Zhang, Phys. Rev. B **57**, R3213(R) (1998).

[30] J. Fernández-Rossier, M. Braun, A. S. Núñez, and A. H. MacDonald, Phys. Rev. B **69**, 174412 (2004).

[31] R. J. Doornenbal, A. Roldán-Molina, A. S. Nunez, and R. A. Duine, Phys. Rev. Lett. **122**, 037203 (2019).

[32] J. Shibata, G. Tatara, and H. Kohno, Phys. Rev. Lett. **94**, 076601 (2005).

[33] A. V. Chumak, P. Dhagat, A. Jander, A. A. Serga, and B. Hillebrands, Phys. Rev. B **81**, 140404(R) (2010).

[34] V. Vlaminck and M. Bailleul, Science **322**, 410 (2008).

[35] I. A. Dzyaloshinsky, J. Phys. Chem. Solids **4**, 241 (1958).

[36] T. Moriya, Phys. Rev. Lett. **4**, 228 (1960).

[37] J.-H. Moon, S.-M. Seo, K.-J. Lee, K.-W. Kim, J. Ryu, H.-W. Lee, R. D. McMichael, and M. D. Stiles, Phys. Rev. B **88**, 184404 (2013).

[38] T. Schneider, A. A. Serga, T. Neumann, B. Hillebrands, and M. P. Kostylev, Phys Rev B **77**, 214411 (2008).

[39] V. E. Demidov, M. P. Kostylev, K. Rott, P. Krzysteczko, G. Reiss, and S. O. Demokritov, Appl. Phys. Lett, **95**, 2509 (2009).

[40] T. Yu and G. E. W. Bauer, in *Chirality, Magnetism, and Magnetoelectricity: Separate Phenomena and Joint Effects in Metamaterial Structures*, edited by E. Kamenetskii (Springer International Publishing, 2021).

[41] T. Wolfram and R. E. De Wames, Phys. Rev. Lett. **24**, 1489 (1970).

[42] B. A. Kalinikos, M. P. Kostylev, N. V. Kozhus, and A. N. Slavin, J. Phys.:Condens. Matter **2**, 9861 (1990).

[43] C. Bayer, J. Jorzick, B. Hillebrands, S. O. Demokritov, R. Kouba, R. Bozinoski, A. N. Slavin, K. Y. Guslienko, D. V. Berkov, N. L. Gorn, and M. P. Kostylev, Phys. Rev. B **72**, 064427 (2005).

[44] T. Yu, C. P. Liu, H. M. Yu, Y. M. Blanter, and G. E. W. Bauer, Phys. Rev. B **99**, 134424 (2019).

[45] S. Klingler, A. V. Chumak, T. Mewes, B. Khodadadi, C.Mewes, C. Dubs, O. Surzhenko, B. Hillebrands, and A. Conca, J. Phys. D **48**, 015001 (2015).

[46] H. C. Wang, J. L. Chen, T. Yu, C. P. Liu, C. Y. Guo, H.Jia, S. Liu, K. Shen, T. Liu, J. Y. Zhang, M. A. Cabero Z, Q. M Song, S. Tu, L. Flacke, M. Althammer, M. Weiler, M. Z. Wu, X. F. Han, K. Xia, D. P. Yu, G. E. W. Bauer, and H. M. Yu, arXiv:2005.10452.

[47] Y. Tserkovnyak and M. Kläui, Phys. Rev. Lett. **119**, 187705 (2017).

[48] Q. Wang, B. Heinz, R. Verba, M. Kewenig, P. Pirro, M. Schneider, T. Meyer, B. Lagel, C. Dubs, T. Bracher, and A. V. Chumak, Phys. Rev. Lett. **122**, 247202 (2019).

[49] See Supplemental Material at [...] for the derivation of interaction Hamiltonian and analysis on the incoherent exchange scattering.

[50] A. A. Abrikosov, L. P. Gorkov, and I. E. Dzyaloshinski, *Methods of Quantum Field Theory in Statistical Physics* (Prentice Hall, Englewood Cliffs, N. J., 1963).

[51] A. Griffin, T. Nikuni, and E. Zaremba, *Bose-Condensed Gases at Finite Temperatures* (Cambridge University Press, Cambridge, England, 2009).

[52] J. D. Jackson, *Classical Electrodynamics* (Wiley, New York, 1998).

[53] P. Lodahl, S. Mahmoodian, S. Stobbe, A. Rauschenbeutel, P. Schneeweiss, J. Volz, H. Pichler, and P. Zoller, Nature (London) **541**, 473 (2017).

[54] I. Bertelli, J. J. Carmiggelt, T. Yu, B. G. Simon, C. C. Pothoven, G. E. W. Bauer, Y. M. Blanter, J. Aarts, and T. van der Sar, Sci. Adv. **6**, eabd3556 (2020).

[55] H. Haug and A. P. Jauho, *Quantum Kinetics in Transport and Optics of Semiconductors* (Springer, Berlin, 1996).

[56] F. Casola, T. van der Sar, and A. Yacoby, Nat. Rev. Mat. **3**, 17088 (2018).

[57] S. O. Demokritov, B. Hillebrands, and A. N. Slavin, Phys. Rep. **348**, 441 (2001).

[58] L. Caretta, E. Rosenberg, F. Bütner, T. Fakhrul, P. Gargiani, M. Valvidares, Z. Chen, P. Reddy, D. A. Muller, C. A. Ross, and G. S. D. Beach, Nat. Comm. **11**, 1090 (2020).

[59] K. Yamamoto, G. C. Thiang, P. Pirro, K.-W. Kim, K. E.-Sitte, and E. Saitoh, Phys. Rev. Lett. **122**, 217201 (2019).